Small-size Dual-band Filters on Capacitively Loaded Cavities

Viacheslav Turgaliev, Dmitry Kholodnyak[1] and Irina Vendik

Microwave Microelectroncs Laboratory, Department of Microelectronics & Radio Engineering, St. Petersburg Electrotechnical University "LETI", 5 Prof. Popov str., 197376, St. Petersburg, Russia

[1] Dmitry.Kholodnyak@mwlab.spb.ru

***Abstract* — The design of dual-band microwave filters using capacitively loaded cavities (CLCs) is presented and discussed. Two different structures of the dual-mode resonators based on two CLCs nested one into another and on combination of a CLC with a complimentary split-ring resonator (CSRR) are considered. Advantages and challenges of the both designs are discussed. Design examples of the advanced resonators and filters implemented in the low temperature co-fired ceramics (LTCC) as well as printed circuit board (PCB) technologies are presented.**

***Index Terms* — Cavity, complimentary split-ring resonator, dual-band filter, low temperature co-fired ceramics, substrate integrated waveguide.**

I. INTRODUCTION

Multi-band microwave devices are highly demanded for modern and future wireless communication systems. Among them, multi-band filters are the mostly required components.

A number of design methods for dual-band microwave filters are known to the date. A dual-band filter can be designed as cascade of a broadband bandpass filter and a bandstop filter [1]. A similar approach deals with introduction of transmission zeroes inside the passband of a broadband filter [2], [3]. Besides, a dual-band filter can be realized as a parallel integration of two bandpass filters [4] or as a structure using interference between the waves propagating in two different ways [5]. Employment of dual-mode resonant structures like a step-impedance resonator is also a widely spread technique to design of dual-band filters [6].

Substrate integrated waveguide (SIW) has recently become a very popular technology for a design of low-profile low-weight microwave filters with a low insertion loss over passband [7], [8].Various designs of dual-band filters in SIW technology have been reported in literature [9], [10]. SIW structures loaded by the complimentary split-ring resonators (CSRRs) are commonly used in these designs [7]-[10].

Based on low-profile waveguide or cavity structures, SIW filters still occupy a rather large area that is mostly remarkable for low-frequency applications.

On the other hand, loading a cavity with a capacitive post can result in a dramatic reduction of resonator size while still maintaining a relatively high unloaded Q-factor [11], [12]. It has been experimentally demonstrated that a highly loaded cavity can be smaller than one eighth of the guided wavelength ($\lambda_g/8$) whereas its Q-factor still remains much higher with respect to conventional quasi-lumped element and transmission line resonators [13].

We have recently introduced a design concept for small-size low-loss dual-band filters based on nested CLCs with different resonant frequencies which can be chosen almost arbitrarily [13]. Moreover, such an approach allows reducing the area occupied by the dual-band filter.

In this paper the design method is discussed in more details and illustrated with some examples. A different design technique is also considered that allows designing dual-band SIW filters based on CLC and CSRR in combination. Advantages and challenges of the both design methods are discussed. The design examples implemented by means of two fabrication technologies: the low temperature co-fired ceramics (LTCC) technology and the printed circuit board (PCB) technology are presented. The results of electro-magnetic simulations are compared with experimental data.

II. ADVANTAGES OF BANDPASS FILTERS ON MINIATURIZED CAPACITIVELY LOADED CAVITIES

The design principle of bandpass filters based on CLCs and their advantages for telecommunication applications are well illustrated by the example presented in Fig. 1.

The three-pole LTCC filter consists of three coupled low-profile cavities operating in the TM_{110} mode. Each cavity is loaded by a conductive post with a capacitive plate at one end (Fig. 1-a). Sidewalls and the square post are formed by rows of stacked via holes. The electric field is concentrated between the capacitive plate and the top of the cavity whereas the magnetic field distribution remains nearly the same as in an unloaded cavity. Hence, the power dissipation in the metallic parts does not change significantly in presence of the load.

The filter resonators are coupled to each other by means of an iris in the mutual sidewall. Though the nature of such a coupling is generally mixed, the main contribution comes from the electric field (i.e., capacitive coupling). The value of the coupling depends on the iris size. The larger the iris size, the tighter is the coupling. The outermost resonators are connected to external circuits by inductive coupling elements. An equivalent diagram of the filter is shown in Fig. 1-b.

The filter with the Chebyshev response was designed for UMTS/LTE-2100 applications (2110-2170 MHz) and embedded in nine layers of DuPont Green Tape™ 951 LTCC ($\varepsilon_r = 7.8$, $\tan\delta = 0.002$). Six of them are 210 µm thick after sintering, two other layers have the thickness of 42 µm, and more one layer has the thickness of 95 µm. Thus, the total height of the LTCC structure is about 1.44 mm. The filter occupies the area of 19 mm × 7 mm ($0.38\lambda_g \times 0.14\lambda_g$).

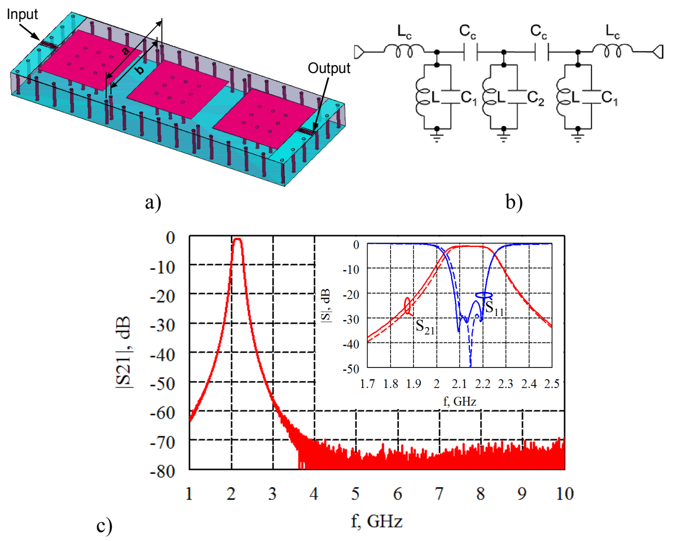

Fig. 1. Three-pole Chebyshev bandpass LTCC filter based on iris-coupled CLCs: (a) structure; (b) equivalent diagram; (c) measured (solid lines) and simulated (dashed lines) characteristics.

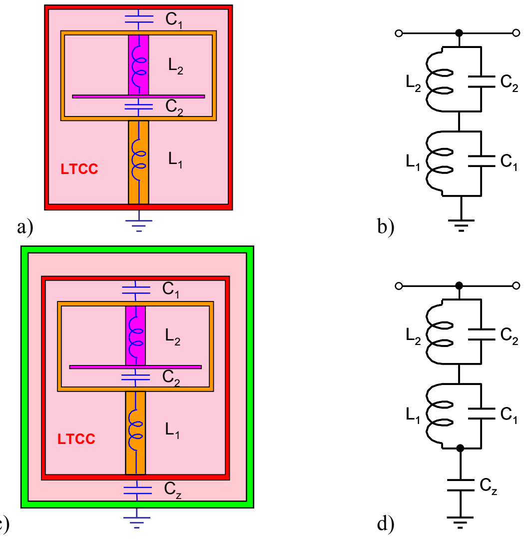

Fig. 2. Two nested CLCs: (a) cross-section of the dual-mode resonator and (b) its equivalent diagram; (c) cross-section of the dual-mode resonator with an additional transmission zero and (d) its equivalent diagram.

The filter characteristics were simulated with the aid of the Ansoft HFSS 3D electromagnetic field solver. The simulated and measured filter performances are plotted in Fig. 1-c. The in-band insertion loss does not exceed 1.2 dB that corresponds to an average unloaded Q-factor of the resonators equal to 150, i.e. at least three times higher than for a quasi-lumped element LTCC resonator. Furthermore, the filter exhibits no spurious response over a wide frequency range (at least up to 10 GHz).

III. Design of Dual-Band Filters Using Capacitively Loaded Cavities

A. *Nested capacitively loaded cavities*

CLCs being of different size and having different resonant frequencies can be nested one into another in such a way that the inner cavity serves as the capacitive load for the outer cavity [13].

Fig. 2-a illustrates a structure of such a matreshka-type dual-mode resonator consisting of two nested CLCs. An equivalent diagram of the resonator is shown in Fig. 2-b. Advantages of the dual-mode resonator of this kind are as follows: i) the resonant frequencies can be chosen almost arbitrarily; ii) a transmission zero is provided between the resonant frequencies; iii) less occupied area compared with two single mode cavities; iv) a sufficiently high Q-factor; v) no spurious response over a wide frequency range.

A transmission zero below every resonant frequency can be easily introduced by surrounding the dual-mode resonator with an external conducting box as shown in Fig. 2-c. The corresponding equivalent diagram is presented in Fig. 2-d.

The frequency behavior of the resonators of both types was analyzed by numerical simulations and confirmed with an experimental investigation (Fig. 3). Test structures of the dual-mode resonators with as non-multiple resonant frequencies as f_{01} = 748 MHz and f_{02} = 1748 MHz were designed and fabricated in the multilayer LTCC technology (Fig. 3-a). Embedded in 16 layers of DuPont Green Tape^{TM} 951, the dual-mode resonator with a transmission zero has the only size of 7.6 mm × 5.2 mm. The height of the LTCC structure is 2.9 mm. The linear size of the resonator does not exceed $\lambda_g/18$ at f_{01} and $\lambda_g/8$ at f_{02}. Simulated and experimentally obtained characteristics of the dual-mode resonators are plotted in comparison in Fig. 3-b and 3-c.

B. *Dual-band filters on nested capacitively loaded cavities*

A structure of coupled dual-mode resonators based on two nested CLCs is schematically shown in Fig. 4-a. The outer cavities are coupled to each other through an iris in the mutual

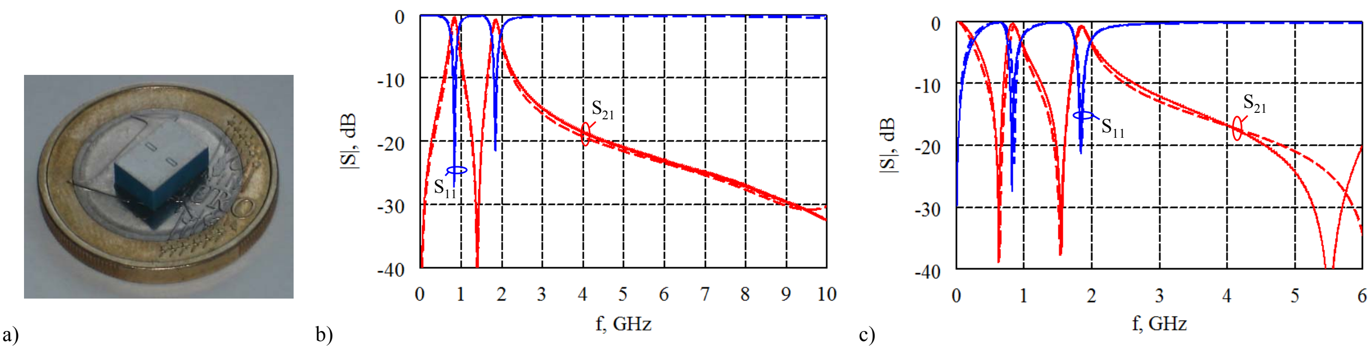

Fig. 3. Dual-mode LTCC resonators on nested CLCs: (a) photograph of a test sample; (b) measured (solid lines) and simulated (dashed lines) characteristics of the resonator; (c) measured (solid lines) and simulated (dashed lines) characteristics of the resonator providing an additional transmission zero.

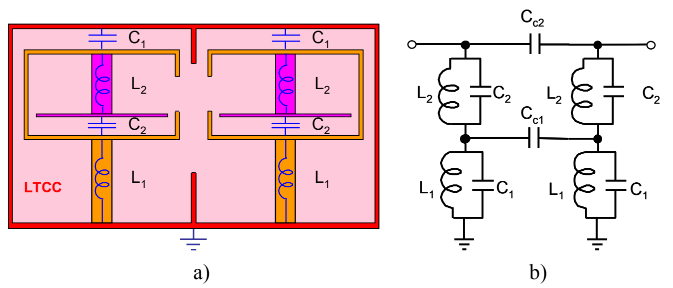

Fig. 4. Coupled dual-mode resonators based on nested CLCs: (a) cross-section of the structure and (b) equivalent diagram.

side wall. Additional irises in the adjacent side walls of the inner cavities are used to provide a coupling between them.

An equivalent diagram of the coupled resonators is presented in Fig. 4-b. The coupling between the tanks with the resonant frequencies f_{01} and $f_{02} > f_{01}$ is represented by the capacitances C_{c1} and C_{c2} of different branches of the circuit. At the frequency f_{01} the two coupling capacitances get connected in parallel, so the total capacitance of the coupling is $C_c(f_{01}) = C_{c1} + C_{c2}$. Meanwhile, at f_{02} the coupling capacitance is $C_c(f_{02}) = C_{c2}$.

The following design method is suggested for the filters based on nested CLCs. As the first step, two single-band filters with the central frequencies f_{01} and f_{02} are designed separately using a conventional synthesis technique. Then the coupling values of the filter designed for f_{01} are corrected as $C'_{c1} = C_{c1} - C_{c2}$. After this, the two filters are integrated as shown in Fig. 4-b. The method can be also used to design dual-band filters with additional transmission zeros based on the resonator structure of Fig. 2-c.

A design example of the three-pole dual-band filter for application at 698–798 MHz and 1710–1788 MHz is demonstrated in Fig. 5. The filter was implemented in the LTCC technology using the above mentioned structure of the dual-mode resonator (Fig. 2-c.). The filter is as small as 12 mm × 7.6 mm, corresponding to only $\lambda_g/12$. It provides a low insertion loss (1.4 dB and 2.1 dB in the lower and higher passbands, respectively) and a high selectivity.

C. Dual band filters on combination of a capacitively loaded cavity and a CSRR

A dual-mode resonator can be designed as a combination of a CLC and a CSRR formed on the cavity top cover (Fig. 6-a). The cavity operates at the lower resonant frequency while the upper resonance is provided by the CSRR. An equivalent diagram of the dual-mode resonator is shown in Fig. 6-b.

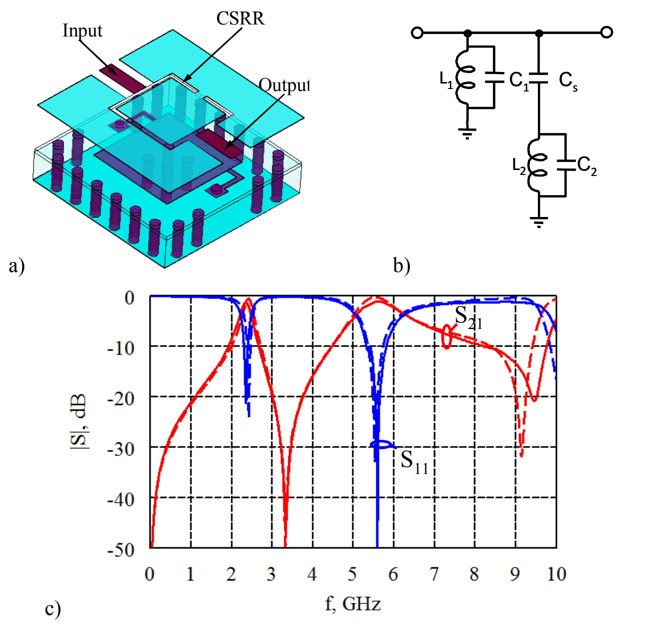

Fig. 6. Dual-mode resonator on combination of a CLC and a CSRR: (a) structure; (b) equivalent diagram; (c) measured (solid lines) and simulated (dashed lines) frequency responses.

The size of such a dual-mode resonator is limited by the dimensions of the single mode cavity. Since the CSRR is a planar structure, its integration with cavity does not result in an increase in height of the structure as for the dual-mode resonator on nested CLCs. However, the unloaded Q-factor of the CSRR is lower in comparison with that of the CLC. Hence, the dual-band resonators of this type can be favourably used when the insertion loss in the upper filter passband is not of a crucial importance e.g. to design filters with the upper fractional bandwidth being wider than the lower one.

Characteristics of the dual-mode resonator with the resonant frequencies of 2.4 GHz and 5.6 GHz are presented in Fig. 6-c. The resonator implemented on 1.7 mm thick two-layer Rogers RO4003 ($\varepsilon_r = 3.55$, $\tan\delta = 0.0027$) PCB occupies the area of 10 mm × 10 mm corresponding to $\lambda_g/8$ at the lower resonant frequency. The unloaded Q-factor is around 130 at the both resonant frequencies.

A coupling between such the dual-mode resonators can be provided in the same way as for the single-mode cavities. Changing the iris size influences the coupling between the CLCs as well as the coupling between the CSSRs. In order to

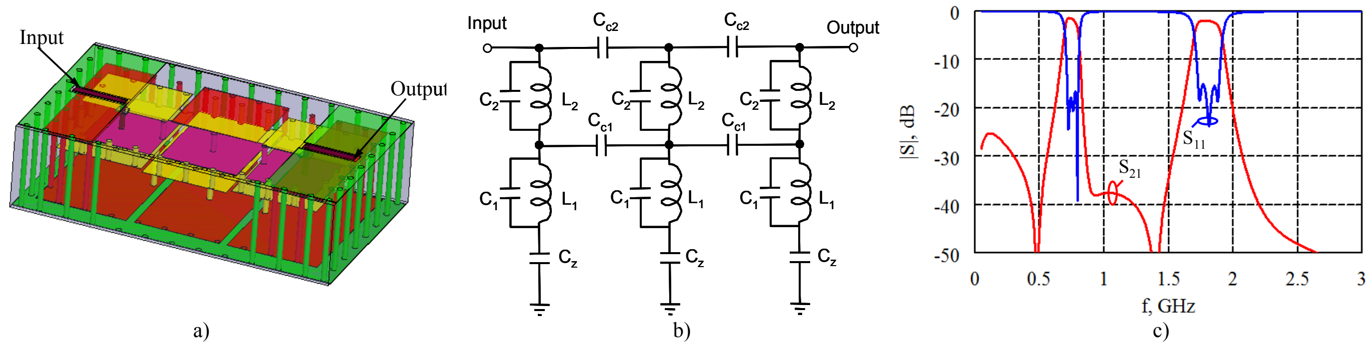

Fig. 5. Three-pole dual-band LTCC filter on nested CLCs: (a) structure; (b) equivalent diagram; (c) characteristics obtained by the full-wave simulation.

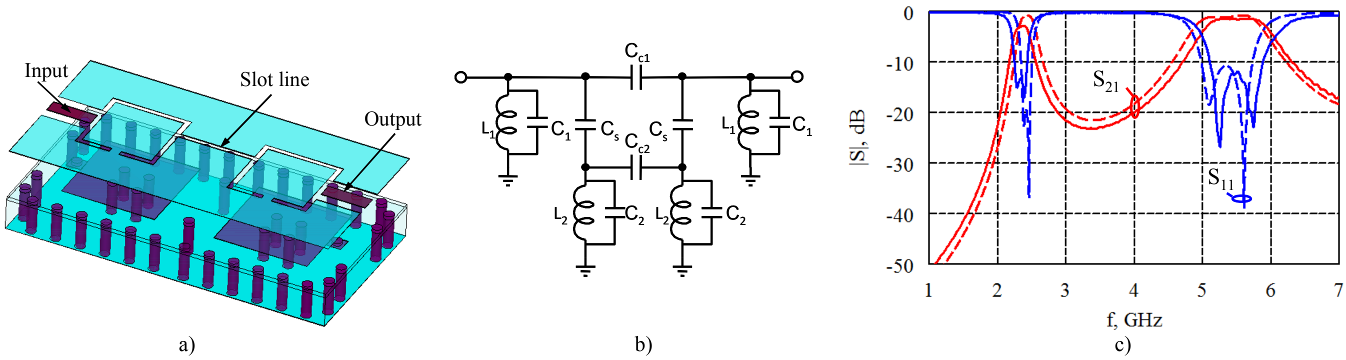

Fig. 7. Two-pole dual-band filter based on CLCs with integrated CSRRs: (a) structure; (b) equivalent diagram; (c) measured (solid lines) and simulated (dashed lines) characteristics.

adjust the coupling between the CSRRs independently, they are connected by a slotline (see Fig. 7-a) providing a tapered coupling whose value depends on a connection point position. An equivalent diagram in illustrated by Fig. 7-b.

A two-pole dual-band filter for WLAN application at 2.3-2.4 GHz and 5.1-5.8 GHz was designed using the resonator structure under consideration (Fig. 7). The filter PCB has the size of 20 mm × 10 mm. The simulated and measured frequency responses of the filter are presented in Fig. 7-c. The experimentally observed operating bandwidths are narrower than the simulated ones that resulted in a slightly increased insertion loss level. The measured insertion loss in the two passbands is 2.5 dB and 1.4 dB, correspondingly.

IV. Conclusions

Small-size low-loss dual-band filters can be designed using the dual-mode resonators based on CLCs. Two different structures of such advanced dual-mode resonators have been considered and applied to the design of dual-band SIW filters for telecommunication applications. A design method for the dual-band filters on nested CLCs has been proposed. A dual-band filter design using CLCs with integrated CSRRs has been discussed as well. The high-performance dual-mode resonators with and without additional transmission zeros and dual-band filters based thereof have been designed and investigated. The experimental characteristics are in good agreement with those predicted by the full-wave simulation that proves the proposed design concept and methods.

Acknowledgement

The work was supported by the MultiWaves Project (PIRSES-GA-2010-247532) of the Seventh Framework Programme (FP7) of the European Commission.

The authors are very grateful to Matthias A. Hein, Stefan Humbla, Dirk Stöpel, and Jens Müller for manufacturing and testing of experimental samples of the LTCC resonators and filter.

The technical support from Rohde-Schwarz company which provided R&S®ZVL vector network analyzer for measurements is gratefully acknowledged.

The useful discussions with Vasa Radonic and Vesna Crnojevic-Bengin are highly appreciated.

References

[1] L.-C. Tsai and C.-W. Hsue, "Dual-band bandpass filters using equallength coupled-serial-shunted lines and Z-transform technique", *IEEE Trans. Microwave. Theory Tech.*, 2004, Vol. 52, No. 4, pp. 1111–1117.

[2] G. Macchiarella and S. Tamiazzo, "Design techniques for dual-passband filters", *IEEE Trans. Microw. Theory Tech.*, 2005, Vol. 53, No. 11, pp. 3265-3271.

[3] M. Sanchez-Renedo and R. Gomez-Garcıa, "Microwave dual-band bandpass planar filter using double-coupled resonating feeding sections", *Proc. of 39th Eur. Microw. Conf.*, Rome, Italy, Sep.-Oct. 2009, pp. 101-104.

[4] C.-F. Chen, T.-Y. Huang, and R.-B. Wu, "Design of dual- and triple-passband filters using alternately cascaded multiband resonators", *IEEE Trans. Microw. Theory Tech.*, 2006, Vol. 54, No. 9, pp. 3550-3558.

[5] Y.-X. Guo, L.C. Ong, M.Y.W. Chia, and B. Luo, "Dual-band bandpass filter in LTCC", IEEE MTT-S Int. Microw. Symp. Dig., 2005, pp. 1-4.

[6] R. Gomez-Garcıa, M. Sanchez-Renedo, B. Jarry, J. Lintignat, B. Barelaud, "Microwave multi-path dual-passband filters for wide-band applications," *Proc. of 39th Eur. Microw. Conf.*, Rome, Italy, Sep.-Oct. 2009, pp. 109-112.

[7] X.-C. Zhang, Z.-Y. Yu, and J. Xu, "Novel band-pass substrate integrated waveguide (SIW) filter based on complementary split ring resonators (CSRRS)", *Progress In Electromagnetics Research*, PIER 72, 2007. pp. 39–46,

[8] Y. Dong, T. Yang, and T. Itoh, "Substrate integrated waveguide loaded by complementary split-ring resonators and its applications to miniaturized waveguide Filters", *IEEE Trans. Microw. Theory Tech.*, 2009, Vol. 57, No. 9, pp. 2211-2223

[9] Y. Dong and T. Itoh "Miniaturized dual-band substrate integrated waveguide filters using complementary split-ring resonators", *IEEE MTT-S Int. Microw. Symp. Dig.*, 2011, pp. 1-4.

[10] Y.Dong, C.-T.M. Wu,; T. Itoh, "Miniaturised multi-band substrate integrated waveguide filters using complementary split-ring resonators", *IET Microwaves, Antennas & Propag.*, 2012, Vol. 6. No. 6, pp. 611-620.

[11] X. Gong, A. Margomenos, B. Liu, W.J. Chappell, and L.P.B. Katehi, "High-Q evanescent-mode filters using silicon micromachining and polymer stereolithography (SL) processing", *IEEE MTT-S Int. Microwave Symp. Dig.*, 2004, pp. 433-436.

[12] P. Ferrand, D. Baillargeat, S. Verdeyme, J. Puech, M. Lahti, and T. Jaakola, "LTCC reduced-size bandpass filters based on capacitively loaded cavities for Q band application", *IEEE MTT-S Int. Microwave Symp. Dig.*, 2005, pp. 1789-1792.

[13] V. Turgaliev, D. Kholodnyak, I. Vendik, D. Stöpel, S. Humbla, J. Müller, and M.A. Hein, "LTCC highly loaded cavities for the design of single- and dual-band low-loss miniature filters", *Proc. of 40th Eur. Microw. Conf.*, Sept.-Oct., 2010, Paris, France, pp. 180-183.